Structures 5 (2016) 67–75

Contents lists available at ScienceDirect

Structures

journal homepage: http://www.elsevier.com/locate/structures

Behaviour of PVC encased reinforced concrete walls under eccentric axial loading

Amr Abdel Havez *, Noran Wahab, Adil Al-Mayah, Khaled A. Soudki [1]

Department of Civil and Environmental Engineering, University of Waterloo, Waterloo, ON, Canada N2L 3G1

ARTICLE INFO

Article history:
Received 7 April 2015
Received in revised form 26 August 2015
Accepted 7 September 2015
Available online 24 September 2015

Keywords:
PVC encased system
Reinforced concrete wall
Polymer
Axial compression
Flexure
Eccentricity

ABSTRACT

Recently, polyvinyl chloride (PVC) has been used as a stay-in-place (SIP) formwork because of its lower cost compared to other materials, durability, and ease to assemble. The PVC SIP formwork used here consists of interconnected elements; panels and connectors that serve as permanent formwork for the concrete walls. In this paper, the behaviour of the PVC encased reinforced concrete walls tested under eccentric compression loading was investigated. The variables were the type of the specimen (PVC encased or control), the longitudinal reinforcement ratio (0.65% or 1.3%) and the eccentricity of the applied load. The PVC encased wall specimens showed superior performance, more ductile and higher capacity when compared to the control wall specimens. An analytical model was developed to predict the ultimate load capacity of the specimens taking into consideration the effect of the PVC on the load carrying capacity of the walls. The calculated and experimental peak loads were in good agreement.

1. Introduction

Recently, polyvinyl chloride (PVC) has been used as a stay-in-place (SIP) formwork because of its lower cost compared to other materials (such as fiber-reinforced polymers), durability, and ease to assemble. This type of formwork has been used mainly for walls in commercial, agricultural and industrial buildings. The PVC stay in place (SIP) formwork is mainly designed to be highly durable in harsh environmental conditions and to enhance the constructability and the mechanical performance of concrete.

The PVC SIP formwork consists of interconnected panels and connectors that serve as permanent formwork for the concrete walls. The panels form the outer shell of the PVC encased wall surface. The connectors slide and interlock with the panels. Panels are connected together via hollow web connectors that hold the form together as shown in Fig. 1. The hollow web connectors allow the concrete to flow laterally between adjacent cells. In addition, it facilitates the placement of reinforcing steel [6]. This system has been commonly used in casting tanks and swimming pools. The PVC encasement system may provide additional tension reinforcement and increase the confinement of the concrete, and hence increase the flexural and axial capacity of the concrete walls. When subjected to flexural load, the increase in the peak load and the ductile response depended on the wall thickness and the reinforcement ratios [3,8,11,12,13]. Under axial load, the effect of the PVC confinement on increasing the ultimate capacity depended on the configuration of the panels and the connectors [5,7,8]. For the plain concrete walls encased with PVC and tested under combined axial and flexure load, the results showed a considerable contribution of the polymer to the tensile load capacity of the specimens [4].

The PVC encased system has been used extensively to form foundation walls, retaining walls, walls in water and waste treatment tanks and walls for swimming pools. In these applications, the walls are resisting axial loads and bending moments. The main objective of this study is to investigate the characteristic behavior of the PVC encased walls with different reinforcement ratios subjected to axial compression and flexural. The behaviour of the PVC encased specimens is compared to the control specimens to assess the contribution of the PVC under different eccentricities and different reinforcement ratios which has not been addressed by existing codes. Then, a theoretical prediction is derived taking into consideration the effect of the PVC on the load carrying capacity of the walls.

2. Experimental program

Eighteen reinforced concrete walls were cast and tested at the structural laboratory at University of Waterloo. The variables in this study were the type of the specimen (PVC encased or control), diameter of the longitudinal reinforcement (10 M or 15 M rebars) resulting in reinforcement ratios of 0.65% and 1.3%, respectively, and the eccentricity of the applied load (33.9 mm, 67.7 mm, 101.6 mm). The eccentricities were proposed as ratios ($^1/_6$, $^1/_3$ and $^1/_2$) of the specimen's thickness. Six specimens acted as control specimens (without PVC encasement) and twelve specimens were PVC encased walls with middle connectors.

* Corresponding author.
E-mail addresses: a4abdelhavez@uwaterloo.ca (A.A. Havez), nwahab@uwaterloo.ca (N. Wahab), aalmayah@uwaterloo.ca (A. Al-Mayah).
[1] Deceased 17 September 2013.

http://dx.doi.org/10.1016/j.istruc.2015.09.003
2352-0124/

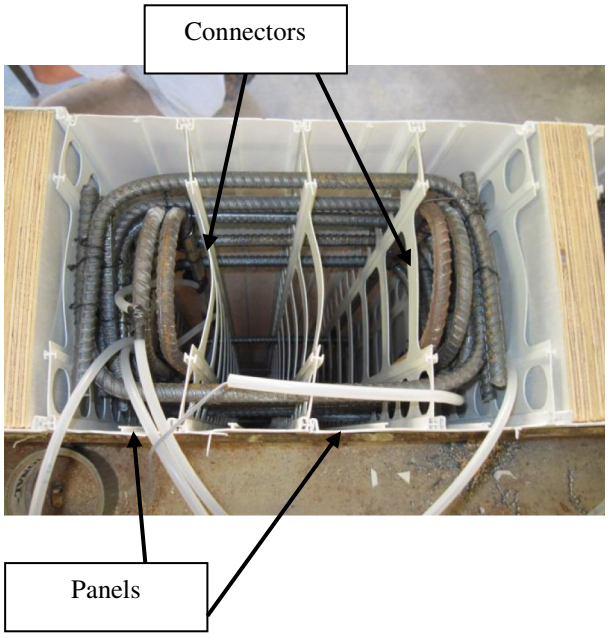

Fig. 1. Top view of a PVC encased wall.

The walls were cast in two batches. In the first batch, the control walls and six PVC encased walls were cast. In the second batch, the remaining PVC encased walls were cast.

All specimens had a rectangular cross section. They were 305 mm wide by 203 mm thick and 1830 mm long. The dimensions of the wall represent a strip in a wall of a tank or a swimming pool with a height that fits the testing frame at University of Waterloo. All the walls were reinforced in the longitudinal direction with 4 steel rebars (10 M or 15 M) as shown in Fig. 2. Two rebars were placed on the tension side and two rebars were placed on the compression side. In the transverse direction, two 10 M stirrups were used at each end of the wall in the first batch and five 10 M stirrups were used at each end of the wall in the second batch to increase the internal confinement and avoid end splitting. Also, the specimens were reinforced with 3 rebars (10 M) in the middle section to simulate the transverse reinforcement used in practice. The longitudinal and transverse reinforcement were tied together using spiral ties. The clear concrete cover on both the tension and the compression sides was 40 mm. Two straight coil loop inserts were used at each end of the wall specimen to facilitate lifting the specimen.

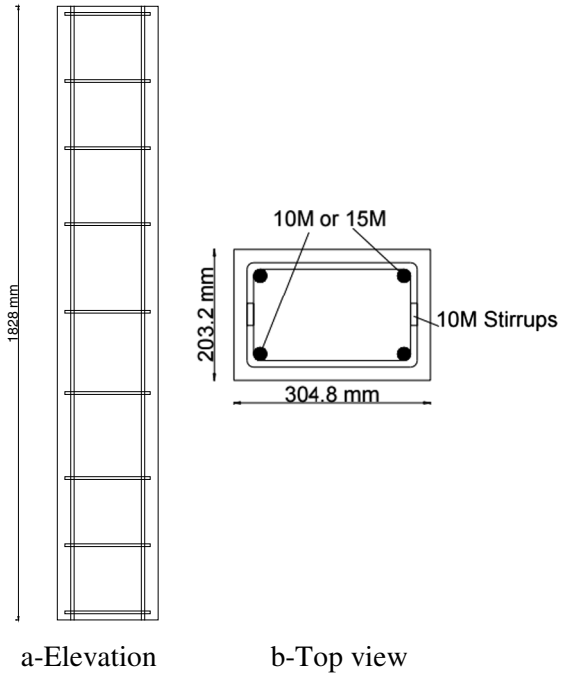

Fig. 2. Reinforcement detailing for the wall specimens.

The PVC encasement consisted of two main elements; panels and middle connectors as shown in Fig. 1. The panels were 150 mm wide and 1.2 mm thick. The middle connectors were 200 mm wide and 1.2 mm thick. Each PVC encased wall consisted of two panels on each face of the wall and five middle connectors. The PVC encased system used here is known commercially as Octaform.

Table 1 shows the test matrix. The notation is as follows; the first letter stands for the wall type; PVC encased wall (O) or control wall (C). The following letter represents the eccentricity, where e6, e3 and e2 represent an eccentricity ratio of $^1/_6$, $^1/_3$ and $^1/_2$ of the specimen's thickness (t), respectively. The last number represents the diameter of the reinforcement rebar. For instance; O-e3-15 is a PVC encased wall reinforced with 4-15 M and subjected to an eccentric compression load applied at $^1/_3$ of the specimen's thickness.

2.1. Material properties

The concrete mix had 10 mm maximum aggregate size. The slump was 170 mm to allow for sufficient flowability of the concrete to fill the cells. The average 28-days compressive strength of the concrete mix used in the first batch was 37.9 MPa and 39.2 MPa for the second batch. According to the manufacturer, the average yield strength of the 10 M and 15 M rebars was 478 MPa and 490 MPa, respectively. The average ultimate strength of the 10 M and 15 M rebars was 702 MPa and 597 MPa, respectively. According to the manufacturer, the ultimate tensile strength of the PVC was 45.9 MPa and the tensile modulus was 2896 MPa. The relationship between the strain (ε_{PVC}) and the stress (f_{PVC}) in the PVC is expressed according to Eq. (1) [13].

$$f_{PVC} = -71518\,\varepsilon_{PVC}^2 + 3412.1\,\varepsilon_{PVC} \quad (1)$$

2.2. Instrumentation and test setup

Strain gauges were mounted on both tension reinforcement and compression reinforcement at mid-span. Furthermore, 5 mm long strain gauges were mounted on the PVC panels at mid-span prior to testing on both compression and tensions sides. Also, a 60 mm long

Table 1
Test matrix.

Specimen	Connector type	Reinforcement	Reinforcement ratio	Eccentricity (mm)	Number of specimens
C-e6-10	NA	4-10 M	0.65	t/6 = 33.9	6
C-e3-10				t/3 = 67.7	
C-e2-10				t/2 = 101.6	
C-e6-15	NA	4-15 M	1.3	t/6 = 33.9	
C-e3-15				t/3 = 67.7	
C-e2-15				t/2 = 101.6	
O-e6-10	Middle	4-10 M	0.65	t/6 = 33.9	12
O-e3-10				t/3 = 67.7	
O-e2-10				t/2 = 101.60	
O-e6-15	Middle	4-15 M	1.3	t/6 = 33.9	
O-e3-15				t/3 = 67.7	
O-e2-15				t/2 = 101.60	

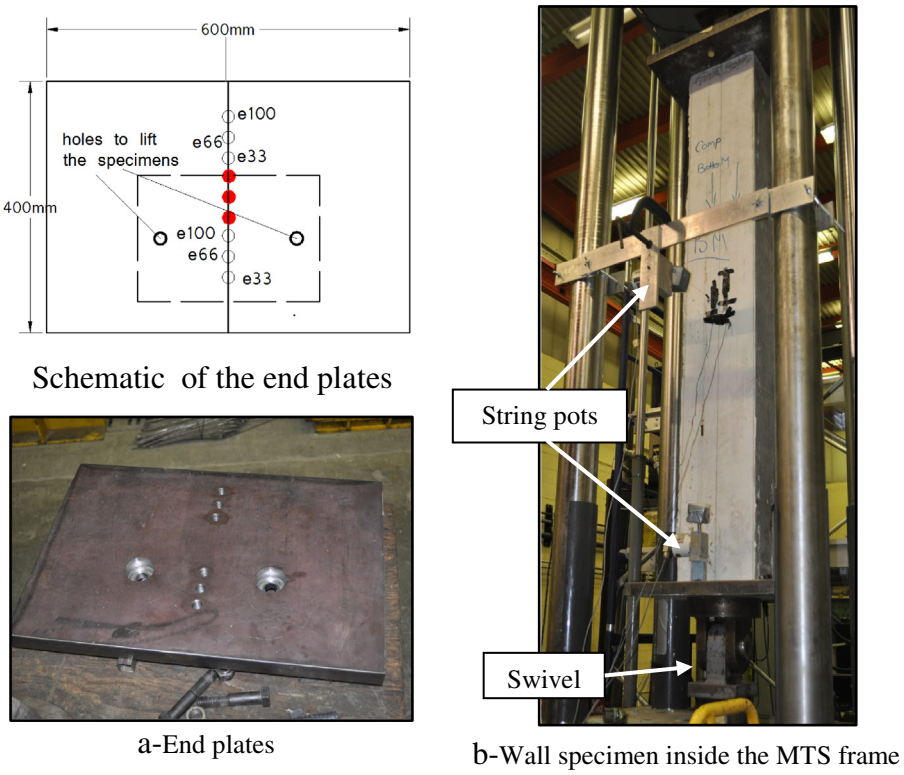

Fig. 3. Wall specimen test setup.

strain gauge was mounted on the concrete compression side of the wall specimen.

To apply the load eccentrically on the wall, a system was used at each end of the wall consisting of a steel plate (Fig. 3-a) and a swivel (Fig. 3-b). The steel plate was 38 mm thick by 400 mm wide by 600 mm long. The plates had six threaded holes to accommodate different eccentricities of the applied load. The plate was placed on the specimen where the dotted line represented the specimen (Fig. 3-a). Hydrostone was used as a filler material between the plate and the specimen to ensure that the ends were perfectly flat and leveled. Threaded rods were used to anchor the plates to the specimens. A swivel system (pin supports) was connected to the movable crosshead and the fixed platen in the testing frame and bolted to the end plates to apply the load at the desired eccentricity. To avoid end failures, additional external confinement was provided at each end using four steel plates (25 mmthick × 200 mm wide) bolted together with high strength bolts forming a collar. The collar counteracted the transverse tensile stresses resulting from the applied compressive stresses in order to avoid premature failure and splitting of the concrete at the ends. It is worth mentioning that four walls were tested without the collar where the failed sections were relatively close from the ends of the wall. Those walls will be referred to as un-confined walls. All the remaining walls were tested with a collar. Further details are reported elsewhere (Havez [1]).

The specimens were tested in a displacement-controlled mode using a servo-hydraulic actuator controlled by a MTS 311 controller. The capacity of the frame was 1500 kN. The load was measured using a load cell attached to the movable crosshead. The displacement was recorded using the internal LVDT. In addition, two string-pots were used to measure the specimen's lateral displacement and the specimen's vertical displacement as shown in Fig. 3-b. To measure the lateral displacement, the string pot was attached to the compression side of the specimen at mid-span. The data was recorded using a data acquisition system. The specimens were loaded monotonically at a rate of 0.5 mm per minute until failure occurred.

3. Test results

3.1. General behaviour

As the specimens were loaded there were three distinct phases. Within the first 3.5 mm deflection (lasted around 7 min), the load increased without any signs of cracking until reaching about 130 kN. Then, it was noticed that the load increased until reaching the peak load within 1 mm deflection (lasted around 1 min). During the testing, close from reaching the peak load, stretch marks appeared on the PVC panels on the tension side near the mid-height or the top section of the encased wall depending on the failure location. At the peak load, crushing of the concrete was observed for the control walls and heard for the encased walls. For the PVC encased walls, crushing of concrete was accompanied with popping sounds of the PVC encasement followed by buckling of the PVC panels. Complete failure of the walls was marked clearly by one or more of the following; crushing of concrete or buckling of the PVC. Past the peak load, the load dropped abruptly and the buckling of the walls, due to the eccentric loading, was noticed. The test continued after the load dropped to assess the effect of the PVC on the post peak response. This phase lasted for 1 to 3 min approximately.

3.2. Modes of failure

Based on the applied eccentricity, the control specimens showed mainly three modes of failure; concrete crushing accompanied with compression steel buckling (Fig. 4, wall reinforced with 10 M and tested at the lowest eccentricity), concrete crushing without yielding of tension steel reinforcement (wall reinforced with 15 M and tested at 67.7 mm eccentricity), and tension steel yielding followed by crushing of the concrete (Figs. 5 and 6, walls reinforced with 15 M and tested at 67.7 or 101.6 mm eccentricity and wall reinforced with 10 M and tested at 101.6 mm). The failed sections for the specimens varied between 300 mm and 1000 mm measured from the top end of the wall (sections

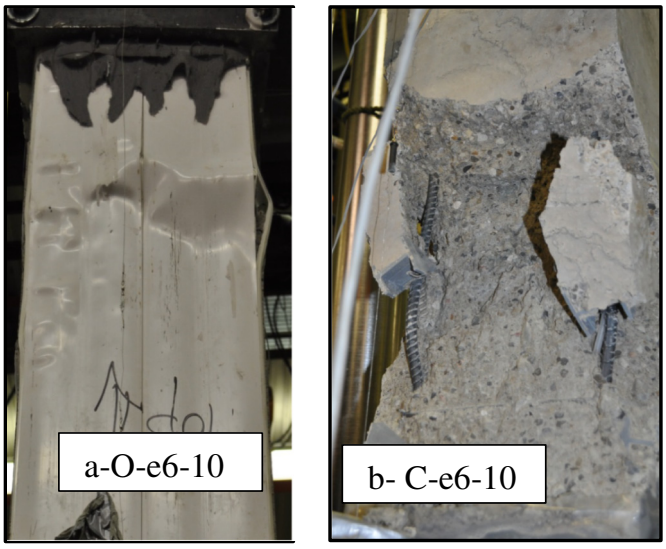

Fig. 4. Failures at the lowest eccentricity (33.9 mm).

last to be filled with concrete during the cast). Failure occurred at these sections due to variation in the compressive strength of the concrete in the upper most portions of the wall where these sections had the lowest compressive strength [9]. This had been confirmed in the current study by flipping some of the wall specimens before testing to ensure that the specimen failed at sections close to the same end (upper end). It is worth mentioning that prior to using the collar, one wall reinforced with 15 M and tested at the lowest eccentricity (33.9 mm) failed by concrete crushing at the end.

The PVC encased specimens showed mainly two modes of failure; concrete crushing followed by PVC buckling or tension steel yielding followed by crushing of the concrete then buckling of the PVC. The walls reinforced with 4-10 M and tested at the lowest eccentricity failed by compression steel yielding followed by concrete crushing then buckling of PVC. The failed section for these walls was at 400 mm from the top end of the wall. At failure, the equivalent control wall specimens experienced significant concrete spalling at the failed section when reaching the ultimate load (Fig. 4-b). However, the PVC encased specimens tested at the same eccentricity did not show any spalling of concrete at ultimate load (Fig. 4-a). It is worth mentioning that at the lowest eccentricity (33.9 mm), regardless of the reinforcement (10 M or 15 M), the unconfined-walls reinforced with 15 M failed by concrete crushing followed by PVC buckling. The failed sections varied between zero and 200 mm from the end of the wall. An additional un-confined wall reinforced with 10 M was tested at the lowest eccentricity. It failed by concrete crushing followed by PVC at sections close to the end of the wall, which empathized the role of the collar in confining the end sections and preventing their failures.

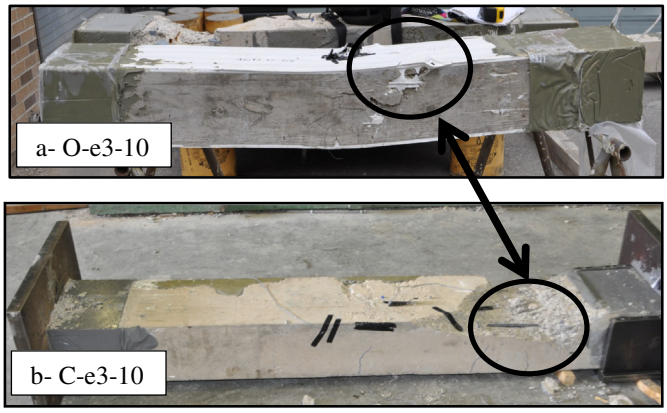

Fig. 5. Failures at the intermediate eccentricity (67.7 mm).

At the intermediate eccentricity (67.7 mm), the PVC encased wall reinforced with 4–10 M failed by tension steel yielding and crushing of the concrete at ultimate load followed by buckling of the PVC (Fig. 5-a). The wall reinforced with 4–15 M failed by crushing of the concrete followed by buckling of the PVC. At the highest eccentricity (101.6 mm), the walls failed by tension steel yielding followed by crushing of the concrete then buckling of the PVC, regardless of the reinforcement (10 M or 15 M) (Fig. 6).

At the lowest eccentricity (33.9 mm), the presence of the PVC encasement did not affect the location of failure. However, for the intermediate eccentricity, the presence of the PVC encasement shifted the failure location towards the mid-span for some specimens. The PVC encased wall reinforced with 10 M failed at 720 mm from the top end of the specimen as opposed to failing at 370 mm from the top end of the specimen for the equivalent control wall. However, for the same specimens reinforced with 15 M, both the control and the PVC encased walls failed almost at the same section (on average 590 mm) from the top end of the specimen. At the highest eccentricity, all control and PVC encased walls failed almost at mid span, regardless of the reinforcement.

3.3. PVC encased walls versus control walls

The PVC encased specimens showed a higher peak load than their peer control walls, further details will be discussed in Section 4. Figs. 7 and 8 show typical test results for a control and a PVC encased wall specimen tested at an eccentricity equal to 67.7 mm. The vertical axis represents the load (kN) and the horizontal axis represents the deflection (mm). All specimens showed the same load versus deflection behaviour. The load increased with deflection until failure where the load dropped abruptly and the deflection increased. It is clear that the PVC encased specimen was stiffer than the control specimens, where the slope of the load versus deflection increased compared to the control specimen. The increase in stiffness was mainly related to the confinement effect of the PVC that opposes the expansion of the concrete. This effect is more pronounced at lower eccentricities and was observed by other researchers [5,7,8].

For both the control and the PVC encased specimens, the behaviour of the load versus strain of steel, concrete and PVC was characterized by an ascending curve until failure where the load dropped with an increase in measured strain, resulting in the descending part of the curve as shown in Figs. 9 and 10. It is clear that at any given load value, the strain gauge readings for the control specimen were higher than the PVC encased specimen, but the PVC encased wall failed at a higher peak load. Therefore, the PVC encased wall can resist the applied load with decreased strain readings compared to the control walls.

4. Discussion

4.1. Peak loads

Table 2 shows the peak load, mid-span deflection and vertical displacement for the control walls and the PVC encased walls. The PVC encased walls reinforced with 4-10 M showed an increase in the peak load of 2.14%, 37.2% and 17.1% at 33.9 mm, 67.7 mm and 101.6 mm eccentricity, respectively over their equivalent confined control specimens. It can be concluded that for the low reinforcement ratio (4-10 M), the effect of the PVC on increasing the axial capacity was noticeable at the high eccentricities (67.7 mm and 101.6 mm). When comparing the PVC encased and control walls at the intermediate eccentricity, it was noticed that the mode of failure shifted from purely

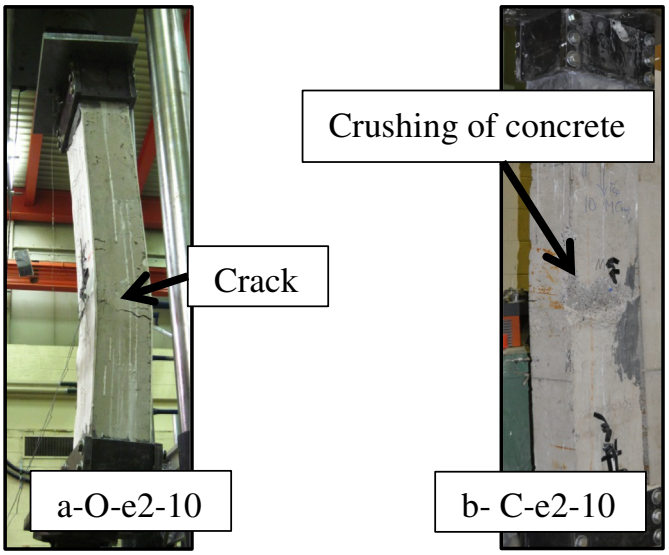

Fig. 6. Failures at the highest eccentricity (101.6 mm).

tension failure to a balanced failure. The tension steel reinforcement in the PVC encased wall yielded right at the ultimate capacity of the wall as opposed to yielding at 94% of the ultimate load for the control specimen resulting in a 34% increase in the ultimate load. The un-confined PVC encased wall reinforced with 4-10 M and tested at the lowest eccentricity (33.9 mm) showed a peak load less than its equivalent confined control and PVC encased walls. This emphasized the effect of the collar on avoiding end failures and developing the full capacity of the wall. In addition, although the same concrete mix was used for the two batches, the two confined PVC encased walls cast in two different batches and tested at an eccentricity of 67.7 mm showed a difference in peak load of 121 kN. The wall tested from the second batch showed a decreased axial capacity. This finding was also consistent for the duplicate PVC encased walls reinforced with 15 M and tested at an eccentricity of 67.7 mm. It is also worth mentioning that the confined control and PVC encased walls tested at an eccentricity of 33.9 mm were cast in two different batches. If both control and PVC encased walls were cast from the same batch, it is expected that the contribution of the PVC would have been higher than the reported value (2.14%).

The PVC encased walls reinforced with 4-15 M showed an increase in the peak load of 10%, 10.34% and 10.67% at 33.9 mm, 67.7 mm and 101.6 mm eccentricity, respectively over their equivalent control walls. It can be observed that the control wall reinforced with 4–15 M and tested at 33.9 mm eccentricity showed a peak load less than its peer specimen reinforced with 4–10 M due to the absence of the confinement system (collar). It is worth mentioning that the two walls reinforced with 15 M and tested at the lowest eccentricity of 33.9 mm were both un-confined. Yet, the PVC encasement enhanced the peak load by 10%. Similar to the duplicate confined specimens cast in two separate batches and reinforced with 4–10 M (O-e3-10), the duplicate confined specimens reinforced with 4–15 M and tested at an eccentricity of 67.7 mm showed a difference in peak load of 79 kN. The peak load of the specimen from the second batch was 79 kN less than the peak load of the specimen from the first batch. It can be concluded that for the high reinforcement ratio (4–15 M), the effect of PVC on increasing the ultimate capacity was much less than the low reinforcement ratio (4–10 M). This indicated that the contribution of the PVC was more significant at lower reinforcement ratios. This finding is consistent with the literature reported on testing the PVC encased walls with different reinforcement ratios under pure bending [12,13].

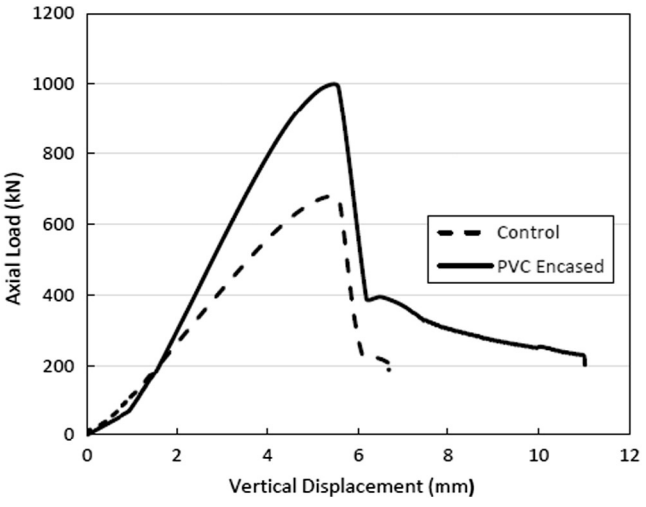

Fig. 7. Typical load versus vertical displacement.

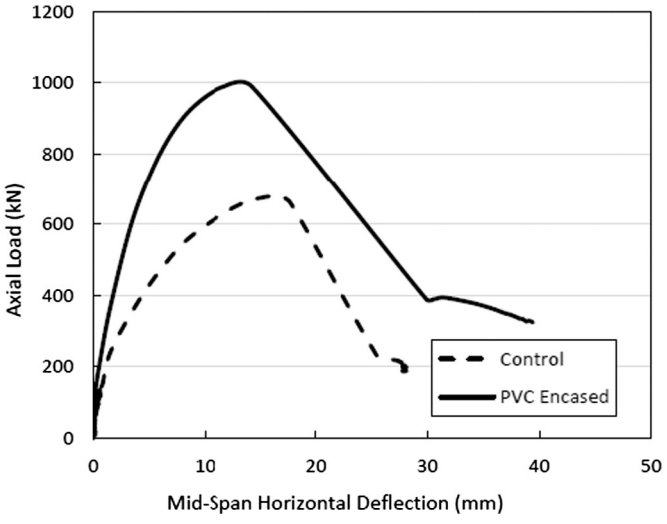

Fig. 8. Typical load versus horizontal displacement.

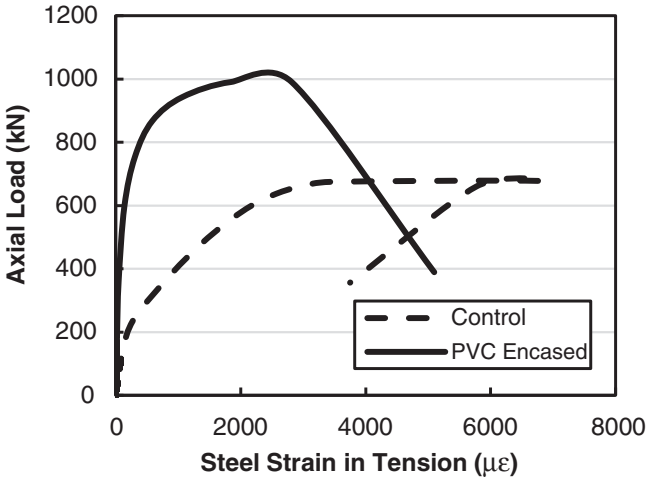

Fig. 9. Load versus tension steel strain for O-e3-10 and C-e3-10 wall specimens.

Table 2
Test results.

	Specimen[b]	Batch	Collar	Peak load (kN)	Mid-span deflection (mm)	Vertical displacement (mm)
4-10 M	C-e6-10	Batch1	Present	1445.1	9	5.1
	O-e6-10	Batch1	Absent	1339.7	5.6	6.8
	O-e6-10	Batch 2	Present	1475.9	7.3	5.7
	C-e3-10	Batch1	Present	677.9	16.4	5.4
	O-e3-10	Batch1	Present	990.3	11.8	5.2
	O-e3-10	Batch 2	Present	869.3	13.4	5.2
	C-e2-10	Batch1	Present	374.8	20.9	5
	O-e2-10	Batch 2	Present	438.9	22.7	5.3
4-15 M	C-e6-15	Batch1	Absent	1266.7	8.3	6.7
	O-e6-15	Batch1	Absent	1393.5	7.5	5.8
	C-e3-15	Batch1	Present	856	15.4	6.3
	O-e3-15	Batch1	Absent	624.6	7.2	4.1
	O-e3-15[a]	Batch1	Present	984	17.2	6.2
	O-e3-15	Batch 2	Present	905	14.3	5.4
	C-e2-15	Batch1	Present	504.1	23.2	7.3
	O-e2-15	Batch 2	Present	557.9	20.3	7

[a] Repeated twice in batch1 due to the premature failure of the specimen during the first test
[b] Two specimens were excluded due to their damage during test setup.

4.2. Effect of eccentricity and reinforcement ratio

For both reinforcement ratios, as the eccentricity increased the peak load of the specimens decreased due to the increase in curvature and the additional moment caused by the eccentric loading. It was noticed that at the same eccentricity the effect of the reinforcement was more noticeable for the control specimens compared to the PVC encased specimens. The control and the PVC encased specimens reinforced with 4–15 M and tested at an eccentricity of 67.7 mm showed an increase in the peak load of 26.3% and 1.6%, respectively, over their peers reinforced with 4–10 M. The difference in the reinforcement effect on the peak load for the control and the PVC encased walls is explained by the different modes of failure. At failure of both the control and the PVC encased walls reinforced with 4–15 M, the concrete crushed without yielding of the tension reinforcement. On the other hand, for the control wall reinforced with 4–10 M, the steel yielded at about 94% of the peak load then the concrete crushed at the peak load. Yet, the PVC encased wall reinforced with 4–10 M failed by steel yielding and concrete crushing at the peak load as explained earlier. For the highest eccentricity (101.6 mm), the control and the PVC encased specimens reinforced with 4–15 M showed an increase in the peak load of 34.5% and 27.1%, respectively, over those reinforced with 4–10 M. The effect of the reinforcement on the peak load is of same order in this case as all the specimens showed the same mode of failure.

4.3. Vertical and mid-span deflection

The PVC encased specimens had almost the same vertical displacement as their equivalent control specimens but at a higher peak load regardless of the reinforcement ratio (Table 2). For both reinforcement ratios (4–10 M and 4–15 M), it was clear that as the eccentricity increased the mid-span deflection at failure increased. However, the PVC encased walls showed almost the same horizontal mid-span deflection at failure as the control walls at different eccentricities.

4.4. Strain profile of PVC walls

The eccentricity of the applied load and the reinforcement ratio were the dominant factors in defining the load-strain behaviour for the wall specimens. All of the specimens (control and PVC encased walls) tested under the lowest eccentricity (33.9 mm) showed a similar load versus strain behaviour in steel, concrete and polymer. Fig. 11 shows typical test results for a confined PVC encased wall specimen reinforced with 4–10 M and tested under the lowest eccentricity. The vertical axis represents the axial load and the horizontal axis represents the strain in all materials. The positive readings indicate tensile strains and the negative readings indicate compressive strains. It is worth mentioning that the readings of the strain gauges were affected by the location of the

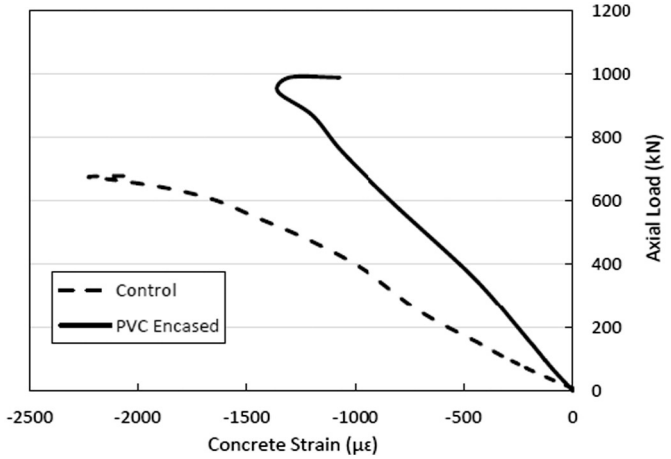

Fig. 10. Load versus concrete strain for O-e3-10 and C-e3-10 wall specimens.

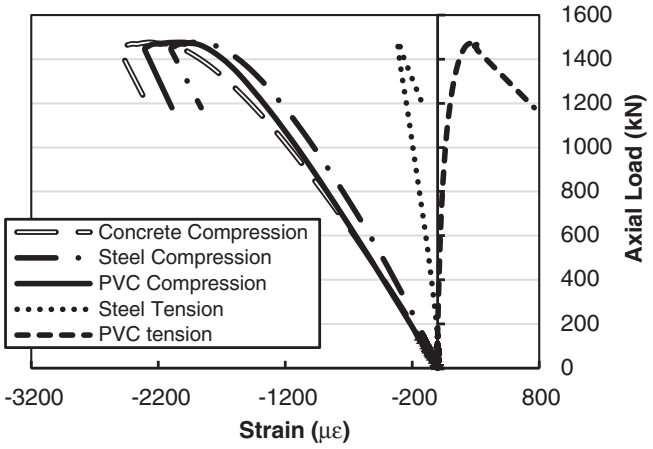

Fig. 11. Load versus strain at mid-span for O-e6-10 wall specimen.

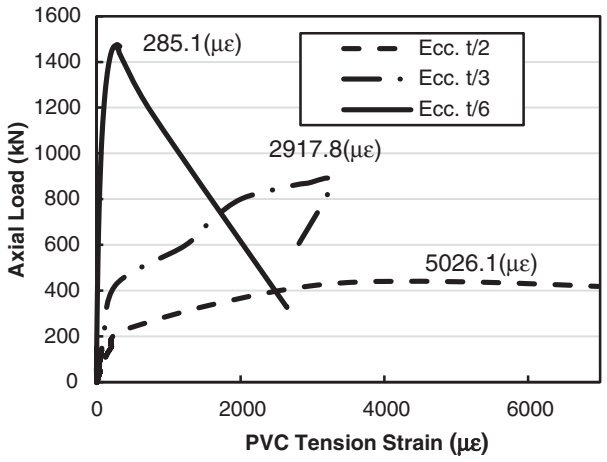

Fig. 12. Load versus PVC strain gauge in tension readings at different eccentricities for the walls reinforced with 4-10 M.

Table 3
Magnification factor for both the control and the PVC encased walls.

	Specimen	Eccentricity (mm)	Experimental peak load (kN)	Moment at mid-span (kN mm)	Moment at the ends (kN mm)	Mag.[a] factor
4-10 M	C-e6-10	33.9	1445.1	61,951.4	48,945.5	1.265
	O-e6-10		1475.9	60,762.8	49,988.73	1.215
	C-e3-10	67.7	677.9	57,031.7	45,914.2	1.242
	O-e3-10		990.3	78,758.6	67,073	1.174
	O-e3-10		869.3	70,526.3	58,877.7	1.197
	C-e2-10	101.6	374.8	45,913	38,079.7	1.205
	O-e2-10		438.9	54,555.3	44,592.3	1.223
4-15 M	C-e6-15	33.9	1266.7	53,416.74	42,903.1	1.245
	O-e6-15		1393.5	57,649.1	47,197.8	1.221
	C-e3-15	67.7	856	57,992.3	54,976.9	1.227
	O-e3-15		624.6	46,801.3	42,304.2	1.106
	O-e3-15		905	74,237.2	61,295.7	1.211
	C-e2-15	101.6	504.1	62,911.7	51,216.6	1.228
	O-e2-15		557.9	68,008	56,682.6	1.199

[a] Stands for magnification factor.

gauge with respect to the failure location. The closer the gauge was to the failure location, the higher the recorded measured readings at failure. From Fig. 11, it is clear that strain gauge readings on both tension and compression steel reinforcement were negative, with lower strain values for the tension steel compared to the compression steel. This indicated that the whole section was under compression at the peak load due to the low applied eccentricity (33.9 mm). Also, the PVC panels on the tension side showed positive strain gauge readings of less than 300 μ-strains.

At the intermediate and highest eccentricity (67.7 and 101.6 mm), the specimens showed a load versus strain behaviour similar to those tested under the lowest eccentricity but with different peak values. The readings of the strain gauges were in a good agreement with the mode of failure for all the specimens.

Fig. 12 compares the typical tension strain gauge readings for the PVC panels at different eccentricities for the walls reinforced with 10 M. The strain gauge readings on the compression side showed the same behaviour. It is clear that the tensile strain gauge readings on the PVC panels increased as the eccentricity increased. Thus, the PVC panels on the tension side showed higher contribution at larger eccentricities where the mode of failure shifted from a compression failure to a tension failure.

5. Theoretical prediction

An analytical model was developed to predict the ultimate load capacity of the specimens taking into consideration the effect of the PVC on the load carrying capacity of the walls. It can also be used to calculate the strains in the concrete and the steel at failure at different eccentricities. The model was based on the equilibrium of forces and the moment magnification factor method, where the effect of secondary stresses associated with the column's deformations were taken into consideration, to predict the peak load.

Cracked sectional analysis was carried out based on the strain and the stress compatibility to define the strength of the section. The failure occurred for the control and the PVC encased wall specimens when the concrete reached the crushing strain in compression (Eq. (2)). The strain in each material (steel, concrete and PVC) at any location was determined by assuming a linear strain distribution as shown in Eq. (3) and Fig. 13. The forces and stresses in the steel reinforcement and the PVC panels were calculated using Eq. (4). Then, the position of the neutral axis (c) was determined using the equilibrium of the internal forces and external forces as shown in Eq. (5).

$$\varepsilon_c = 0.0035 \tag{2}$$

$$\frac{\varepsilon_c}{c} = \frac{\varepsilon'_c}{c'} = \frac{\varepsilon'_s}{c-d'} = \frac{\varepsilon_s}{d-c} = \frac{\varepsilon_{PVC}}{h-c} \tag{3}$$

$$\begin{aligned} C_c &= \alpha_1 f'_c b \beta_1 c \\ C_s &= \varepsilon'_s E_s A'_s \quad \varepsilon'_s < \varepsilon_y \\ C_s &= f_y A'_s \quad \varepsilon'_s \geq \varepsilon_y \\ T_s &= \varepsilon_s E_s A_s \quad \varepsilon_s < \varepsilon_y \\ T_s &= f_y A_s \quad \varepsilon_s \geq \varepsilon_y \\ T_{PVC} &= A_{PVC} f_{PVC} \end{aligned} \tag{4}$$

$$\begin{aligned} P &= C_c + C_s - T_s - T_{PVC} \\ M &= C_c\left(\frac{h}{2} - \beta_1 \frac{c}{2}\right) + C_s\left(\frac{h}{2} - d'\right) + T_s\left(\frac{h}{2} - d\right) + T_{PVC}\left(\frac{h}{2}\right) \end{aligned} \tag{5}$$

where C_c = the concrete compression force (N), C_s = the steel compression force (N), ε'_s = the strain in the compression steel, ε_s = strain in the tension steel, T_s = steel tension force (N), A_{PVC} = area of the PVC (mm^2), A_s = area of the tension steel (mm^2), A'_s = area of compression steel (mm^2), h = depth of the section (mm), c = position of the neutral

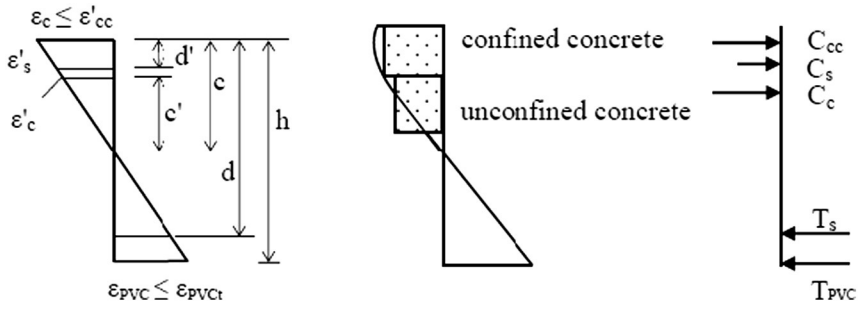

Fig. 13. Strain, stress and internal force distribution for PVC encased specimens subjected to combined flexure and axial load.

Table 4
Calculated peak loads with confinement effect.

	Specimen	Batch	Collar	Experimental peak load (kN)	With confinement		Without confinement
					Theoretical peak load (kN)	Percentage difference (%)	Theoretical peak load (kN)
4-10 M	C-e6-10	Batch1	Present	1445.1	1145.23	20.8	1145.23
	O-e6-10	Batch1	Absent	1339.7	–	–	–
	O-e6-10	Batch 2	Present	1475.9	1367	7.3	1148.5
	C-e3-10	Batch1	Present	677.9	654.26	3.5	654.26
	O-e3-10	Batch1	Present	990.3	786	15.5	669
	O-e3-10	Batch 2	Present	869.3			
	C-e2-10	Batch1	Present	374.8	356.58	4.9	356.58
	O-e2-10	Batch 2	Present	438.9	427.5	2.6	381.6
4-15 M	C-e6-15	Batch1	Absent	1266.7	1271.9	0.41	1271.9
	O-e6-15	Batch1	Absent	1393.5	1494.8	7.8	1274.3
	C-e3-15	Batch1	Present	856	789.69	7.74	789.69
	O-e3-15	Batch1	Absent	624.6	–	–	–
	O-e3-15[a]	Batch1	Present	984	950.3	0.61	794.5
	O-e3-15	Batch 2	Present	905			
	C-e2-15	Batch1	Present	504.1	497.41	1.32	497.41
	O-e2-15	Batch 2	Present	557.9	569.7	2.1	510.9

[a] An average value of the peak load was used for duplicate specimens.

axis (mm), T_{PVC} = PVC tension force (N), d' = depth of the compression steel (mm), P = axial capacity of the section (N), M = moment of resistance of the section (N.mm).

In this study, when the confinement effect was initially taken equal to zero (concrete crushing strain equals 0.0035), the calculated results were too conservative (see Table 4). Based on the literature, the confinement effect under concentric axial load for the same PVC encasement used here was about 20% [5,7,8]. In the current study, the load was applied at different eccentricities. It is expected that the confinement effect decreases as the eccentricity increases [10]. Pham et al. [10] reported a reduction in the confinement effect by 40% when the eccentricity was increased from zero to 25 mm (1/6 of the specimen's thickness). Due to the lack of data of PVC encased walls, the confinement effect of the PVC was approximately estimated to increase the axial load capacity by 10% at all eccentricities. Hence, the strength of the confined concrete (f'_{cc}) was taken equal to $1.1f'_c$. Further details about the estimated concrete strength can be found in Havez [1]. (6) shows the confined concrete strain.

The forces in the PVC and steel were estimated using Eq. (4). However, the force in the concrete was divided into the force in the confined concrete (C_{cc}) and un-confined concrete (C_c) (Eq. (7)). The position of the neutral axis (c) and the applied load (P) can be determined using the equilibrium of the internal and external forces (Eq. (8)).

$$\varepsilon'_{cc} = \left(5\left[\frac{f'_{cc}}{f'_c} - 1\right] + 1\right) * (\varepsilon_c) \text{for PVC encased specimens} \tag{6}$$

$$C_{cc} = \phi_c \frac{f'_c + f'_{cc}}{2} b\left[C - \frac{c}{\varepsilon'_{cc}}\varepsilon'_c\right]$$
$$C_c = \phi_c \alpha_1 f'_c b \beta_1 \left[\frac{c}{\varepsilon'_{cc}}\varepsilon'_c\right] \tag{7}$$

$$P = C_{cc} + C_c + C_s - T_s - T_{PVC}$$
$$M = C_{cc}\left(\frac{h}{2} - \left[c - \frac{C}{\varepsilon'_{cc}}\varepsilon'_c\right]\frac{2f'_c + f'_{cc}}{3f'_c + 3f'_{cc}}\right) + C_c\left(\left[\frac{h}{2} - C\right] + \left[1 - \frac{\beta_1}{2}\right]\left[\frac{C}{\varepsilon'_{cc}}\varepsilon'_c\right]\right)$$
$$+ C_s\left(\frac{h}{2} - d'\right) + T_s\left(\frac{h}{2} - d\right) + T_{PVC}\left(\frac{h}{2}\right) \tag{8}$$

The moment magnification method was used to magnify the end moments to account for the secondary stresses and include the P–Δ effect as shown in Eq. (9) [4]. The Euler buckling load and the inertia of the cross section of the concrete column was calculated using (10) and (11), respectively [2].

$$M_c = magnification\,factor \times M$$
$$M_c = \frac{1}{1 - \frac{P}{P_c}} M \tag{9}$$

$$P_c = \frac{\pi^2 EI}{(Kl_u)^2} \tag{10}$$

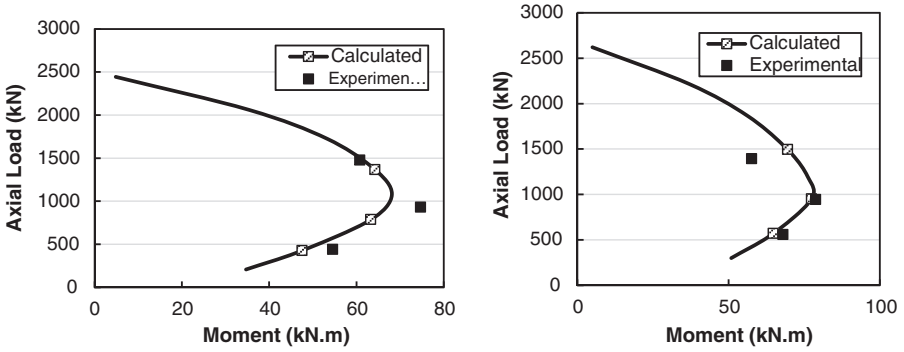

a-Walls reinforced with 4-10M b-Walls reinforced with 4-15M

Fig. 14. Interaction diagram for PVC encased walls.

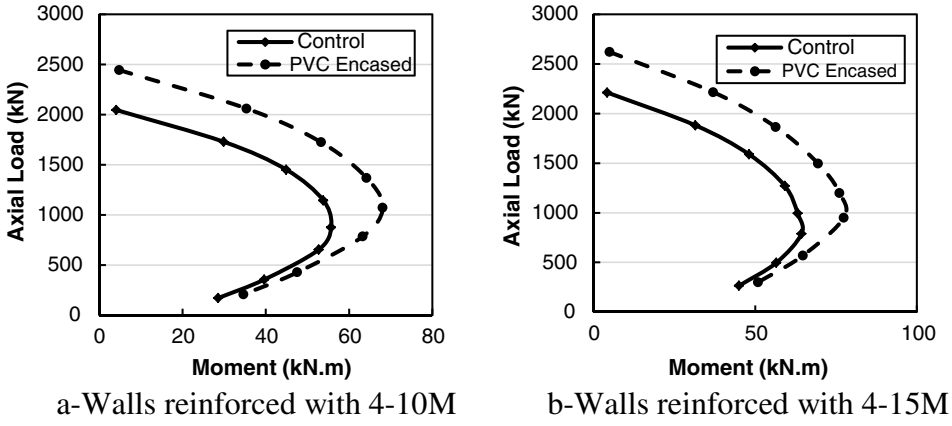

Fig. 15. Calculated interaction diagrams for both control and PVC encased walls.

$$EI = \frac{0.2E_cI_g + E_sI_{st}}{1+\beta_d} \tag{11}$$

where M is the maximum moment due to applied loads but not including P–Δ effect (N mm); M_c, applied moment (N mm); P_c, Euler buckling load (N); P, axial load applied at the ends of the walls (N); l_u, is the unsupported length of the specimen; E, Young's modulus; I, the moment of inertia of the cross section; E_c, concrete modulus of elasticity (N/mm^2); E_s, steel modulus of elasticity (N/mm^2); I_g, moment of inertia of the gross section(mm^4); I_{st}, moment of inertia of reinforcement about the cross-sectional centroid (mm^4); β_d, ratio of the maximum factored axial dead load to the total factored axial load; and k, effective length factor for columns.

The magnification factor is the ratio between the total moment at mid-span to the end applied moment. Therefore, the experimental magnification factor for the wall specimen was calculated using the experimental mid span deflection, applied eccentricity at the wall's end and peak loads. The results are provided in Table 3. It was noticed that for a given reinforcement ratio and eccentricity, the magnification factor for the control and the PVC encased walls was almost the same. Therefore, for any PVC encased wall, the magnification factor was taken equal to its peer control wall.

The peak load was calculated for all the PVC encased specimens. The results are presented in Table 4. Fig. 14 shows the calculated and the experimental interaction diagrams for all the PVC encased specimens. Fig. 15 shows the calculated interaction diagram for all the specimens (control and PVC confined specimens). The calculated capacities showed better correlation with the experimental peak loads when the confining effect of the PVC was taken into consideration than the case with zero confinement. The difference between the experimental and the calculated load was 5.9% on average (15.5% maximum).

6. Conclusion

The following conclusions can be drawn from the work presented here:

1. The PVC encased specimens showed a higher peak load than their peer control walls. The effect of the PVC encasement on increasing the ultimate capacity at a given eccentricity was more significant for the walls reinforced with 4-10 M than the walls reinforced with 4–15 M. For a given reinforcement ratio, the PVC effect on the concrete encasement was more pronounces as the eccentricity increased.
2. The control walls failed by yielding of the steel followed by crushing of the concrete, or by crushing of the concrete without yielding of the steel. For the PVC encased walls, buckling of the PVC occurred after the concrete crushed.
3. The control walls and their peer PVC encased walls showed the same mode of failure except for the control and the PVC encased walls reinforced with 4–10 M and tested at 67.7 mm eccentricity. This is due to shifting the mode of failure from tension failure (steel yielding then concrete crushing) for the control walls to close to the balanced failure (steel yielding and concrete crushing) for the PVC encased walls.
4. Both the control and PVC encased specimens showed the same load versus deflection behaviour. The PVC encased specimens were stiffer than the control specimens, where the slope of the load versus deflection increased for the vertical and the mid-span deflection, the PVC encased specimens and the control specimens showed the same values at failure but the PVC encased walls failed at a higher load.
5. Sectional analysis based on the moment magnification factor was carried out to calculate the capacity of the walls. The calculated capacities showed better correlation with the experimental peak loads when the confining effect of the PVC was taken into consideration than the case with zero confinement.

References

[1] Havez AA. Behaviour of PVC encased reinforced concrete walls under eccentric axial loading. Ontario, Canada: University of Waterloo; 2014.
[2] Canadian Standards Association (CSA). Design of concrete structures. CSA A23.3; 1994.
[3] Chahrour A, Soudki K, Straube J. RBS polymer encased concrete wall. Part I: experimental study and theoretical provisions for flexure and shear. Constr Build Mater 2005;19(7):550–63.
[4] Chahrour A, Soudki K. RBS polymer encased concrete wall part II: experimental study and theoretical provisions for combined axial compression and flexure. Constr Build Mater 2006;20(10):1016–27.
[5] Gupta R. Evaluation of the compressive strength behaviour of the octaform concrete forming system (Phasell). Vancouver, BC: Octaform System Inc.; 2009.
[6] Octaform. Construction guide: version 2 updated 2010. Vancouver, BC: Octaform System Inc.; 2010.
[7] Kuder K. Effect of PVC Stay-in-place formwork on the mechanical performance of concrete. Vancouver, BC: Octaform System Inc.; 2006 103.
[8] Kuder K, Rishi G, Harris-Jones C, Hawksworth R, Henderson S, Whitney J. Effect of PVC stay-in-place formwork on mechanical performance of concrete. J Mater Civ Eng 2009;21(7):309–15.
[9] Petersons N. Strength of concrete in finished structures. Stockholm. Sweden: Elanders Boktryckeri Aktiebolag; 1964.
[10] Pham TM, Lei X, Hadi MNS. Effect of eccentric load on retrofitted reinforced concrete columns confined with FRP. 22nd Australasian Conference on the Mechanics of Structures and Materials (ACMSM22). London: Taylor & Francis Group; 2013. p. 139–44.
[11] Richart FE, Brandtzaeg A, Prown RL. A study of the failure of concrete under combined compressive stress. Bulletin No. 190. Urbana: Engineering Experiment Station, University of Illinois; 1928[103 pp.].
[12] Rteil A, Soudki K, Richardson D. Flexural behavior of octaform™ forming system. ACI SP. St. Louis: ACI SP; 2008 CD format.
[13] Wahab N, Soudki K. Flexural behaviour of PVC stay-in-place formed RC walls. Constr Build Mater 2013;48:830–9.